Chemical pressure effect on bandwidth and dimensionality of quasi-one-dimensional organic conductors: $(DMET)_2X$ [$X=Au(CN)_2$, AuI_2, $AuCl_2$, IBr_2, I_3, $AuBr_2$, and SCN]

Harukazu Yoshino* and Keizo Murata
Department of Molecular Materials Science, Graduate School of Science, Osaka City University, 3-3-138 Sugimoto, Sumiyoshi, Osaka 558-8585, Japan

Kazuya Saito
Research Center for Molecular Thermodynamics, Graduate School of Science, Osaka University, 1-1 Machikaneyama, Toyonaka 560-0043, Osaka, Japan

Hiroyuki Nishikawa, Koichi Kikuchi, and Isao Ikemoto
Department of Chemistry, Graduate School of Science, Tokyo Metropolitan University, 1-1 Minami-Osawa, Hachioji, Tokyo 192-0397, Japan

(Received 15 July 2002; published 21 January 2003)

Thermopower is systematically studied for quasi-one-dimensional (Q1D) organic conductors $(DMET)_2X$ [$X=Au(CN)_2$, AuI_2, $AuCl_2$, IBr_2, I_3, $AuBr_2$ ($Z=1$), and SCN]. The field-orientation dependence of magnetoresistance of $(DMET)_2AuCl_2$ was measured by rotating magnetic field within its most conducting plane and the third angular effect (TAE) was observed at and below 4.2 K. Bandwidth estimated from the thermopower and its anisotropy (or dimensionality) from TAE are compared among $(DMET)_2X$ to discuss chemical pressure effect on the low temperature state of Q1D conductors. It was found that bandwidth varies drastically (25 %) by changing the counter anions, while the dimensionality is almost the same for $(DMET)_2AuBr_2$, $(DMET)_2AuCl_2$, and $(DMET)_2I_3$, which show different temperature dependence of the electric resistivity at low temperature from one another. An analytical formula is presented for the thermopower of dimerized one-dimensional (1D) metals within the tight-binding and the relaxation time approximations. It is shown that the effect of the dimerization is small on magnitude and sign of the thermopower of 1/4-filled 1D metals, while large deviation from the uniform case is predicted if band filling is changed. An approximate simple expression is also given for the angular width of the TAE anomaly as a function of the anisotropy of the transfer integrals and the lattice constants of a triclinic crystal for easy application of this new method.

DOI: 10.1103/PhysRevB.67.035111 PACS number(s): 71.30.+h, 72.15.Gd, 72.15.Jf

I. INTRODUCTION

DMET [dimethyl(ethylenedithio)diselenadithiafulvalene] is a hybrid organic donor made of each half of TMTSF (tetramethyltetraselenafulvalene) and BEDT-TTF [bis(ethylenedithio)tetrathiafulvalene], both of which have provided a variety of organic superconductors. DMET constructs conducting radical salts with inorganic monovalent anions such as PF_6^-, BF_4^-, I_3^-, and so on. Among them the salts of the linear anions $(DMET)_2X$ [$X=Au(CN)_2$, AuI_2, $AuCl_2$, $AuBr_2$ ($Z=1$), I_3, IBr_2, SCN, I_2Br] (Refs. 1,2) constitute a group of quasi-one-dimensional (Q1D) metals whose crystal structures and physical properties are similar to $(TMTSF)_2X$, ($X=PF_6$, ClO_4, and so on). Three kinds of ground states, namely, semiconducting spin-density wave (SDW) [$X=Au(CN)_2$ (Refs. 3,4) and AuI_2 (Ref. 4)], superconducting [$AuCl_2$,[5] I_3, and IBr_2 (Ref. 6)] and metallic ones [$AuBr_2$ ($Z=1$),[7] I_2Br,[6] and SCN (Ref. 1)] are observed for $(DMET)_2X$ at ambient pressure, while $(TMTSF)_2X$ is intrinsically at the SDW state at low temperature and shows superconductivity only under pressure.[8] One should note that the ambient pressure superconductivity of $(TMTSF)_2ClO_4$ does not occur when the anion-ordering transition at 24 K, which results in reconstruction of the Fermi surface, is inhibited by rapid cooling.[9–11] Thus the Q1D DMET salts are considered to be suitable for studying the so-called ''chemical pressure'' effect on the ground state of the Q1D conductors by anion substitution.

Since the suppression of the SDW in $(TMTSF)_2X$ by hydrostatic pressure is well explained by the ''standard theory'' of the SDW transition by Yamaji,[12,13] the effect of both hydrostatic and chemical pressure is often understood as the increase in dimensionality of the Q1D Fermi surface resulting in its worse nesting. Here the dimensionality refers to the anisotropy of the transfer integral ($|t_y/t_x|$) within the most conducting **xy** plane, where **x**, **y**, and **z** are the first, second, and third conducting axes and correspond to **a**, **b**, and **c** in $(TMTSF)_2X$ and to **b**, **a**, and **c** in $(DMET)_2X$, respectively. Our recent uniaxial strain study,[14] however, revealed that the SDW transition of $(TMTSF)_2PF_6$ is suppressed not only by the $\mathbf{y}'$-axis strain but also by that along **x** and **z*** axes, respectively. Since the **x** strain is considered to increase the absolute value of bandwidth or $|t_x|$ but not dimensionality, the uniaxial strain study suggests the importance of $|t_x|$ as a key parameter to determine the ground state of the Q1D system. Indeed Miyazaki *et al.*[15] theoretically showed that the increase in $|t_x|$ results in the decrease in the density of state at Fermi energy and makes the SDW phase unstable. Thus it is necessary to determine experimentally not only the dimensionality but also the magnitude of the bandwidth to eluci-

date the key parameter of the suppression of the SDW transition. For this purpose we propose a new combinational method to determine both of the absolute value of bandwidth and its anisotropy (or dimensionality) of the Q1D metals by measuring thermopower and magnetoresistance.

We have utilized thermopower to estimate $|t_x|$ of the metallic Q1D DMET salts. Thermopower of $(DMET)_2I_3$ (Ref. 16) was reported previously as well as other DMET salts containing semiconducting Q1D salts such as $(DMET)_2PF_6$ and a κ-type quasi-two-dimensional salt $(DMET)_2AuBr_2$ ($Z=2$) that is a polymorph of Q1D $(DMET)_2AuBr_2$ ($Z=1$).[7] An improved sample holder than that in the previous study was used for more precise measurement below 80 K in the present study. By using this holder, thermopower of $(DMET)_2Au(CN)_2$ and $(DMET)_2AuI_2$ was measured and the large critical anomaly probably due to the fluctuation of the SDW transition, which was also pointed out by the Hall effect study,[17] was reported.[18] In addition to these salts, we present the thermopower of the I_3, IBr_2, I_2Br, $AuCl_2$, $AuBr_2$ ($Z=1$), and SCN salts and estimate $|t_x|$ from its temperature dependence in this study.

We also compare $|t_y/t_x|$ of $(DMET)_2I_3$, $(DMET)_2AuBr_2$, and $(DMET)_2AuCl_2$, each of which shows different temperature dependence of the electric resistivity from one another at low temperature. $(DMET)_2I_3$ and $(DMET)_2AuBr_2$ are metallic and the former becomes superconducting at 0.47 K at ambient pressure.[1,2,6] $(DMET)_2AuCl_2$ is also metallic but shows the very slight resistivity upturn around 3 K and undergoes the superconducting transition at 0.83 K.[1,2,5] By considering that $(DMET)_2Au(CN)_2$ and $(DMET)_2AuI_2$ undergo the SDW transition, the resistivity upturn of $(DMET)_2AuCl_2$ is probably the trace of the SDW transition. The salt is, therefore, at the phase boundary between the SDW and superconducting phases in the generalized pressure-temperature phase diagram similar to that of $(TMTSF)_2X$ and their analogs[19] and it is important to estimate the dimensionality of $(DMET)_2AuCl_2$. It must be noted that $(DMET)_2AuCl_2$ is not isostructural to the other DMET salts studied.[20] It will however, be shown later that the electronic state of $(DMET)_2AuCl_2$ is very similar to that of $(DMET)_2I_3$, $(DMET)_2AuBr_2$ ($Z=1$), and $(DMET)_2AuI_2$ in the metallic state and comparison of the band parameters is possible among the salts.

The dimensionality of $(DMET)_2I_3$ and $(DMET)_2AuBr_2$ was previously studied by utilizing the third angular effect (TAE) of magnetoresistance of Q1D metals.[21,22] The TAE is observed in the angular dependence of the magnetoresistance on rotating the magnetic field around the $\mathbf{z}^*$ axis, while the first and second effects of ''Lebed resonance''[23–29] and ''Danner-Kang-Chaikin oscillation''[30] are observed for the rotation around the $\mathbf{x}$ and $\mathbf{y}'$ axes, respectively. In TAE two local minima of the magnetoresistance develop when the field direction is close to the inflection angles of the Q1D Fermi sheet.[31–36] The TAE was first observed for $(DMET)_2I_3$ (Ref. 21) and also found for the relaxed (R) state of $(TMTSF)_2ClO_4$ (Ref. 31) and $(TMTSF)_2PF_6$ under pressure.[34] The TAE is closely related to the warping of Q1D Fermi sheet and, therefore, the dimensionality, $|t_y/t_x|$ can be estimated from the angular width, $\Delta\phi$ of the anomaly. For $(DMET)_2I_3$ and $(DMET)_2AuBr_2$, the experimentally obtained values of $\Delta\phi=28°$ and 27° give $|t_y/t_x|=1/9.7$ and 1/10, respectively.[22] In this study, the TAE is measured for $(DMET)_2AuCl_2$ and its dimensionality is compared with that of $(DMET)_2I_3$ and $(DMET)_2AuBr_2$ as well as $|t_x|$.

II. EXPERIMENTAL

Single crystals of the DMET salts are obtained by the usual chemical oxidation method described elsewhere.[3,5–7] All the crystals are black plate-like with typical dimensions of $0.7\times0.1\times0.03$ mm^3.

Thermopower was measured along the most conducting $\mathbf{x}$ axis. Each sample was mounted on the copper blocks with thermal and electric contacts by using carbon paste. Temperature difference (ΔT) was controlled step-by-step and thermoelectric power (ΔE) was measured simultaneously. The maximum temperature difference was typically 0.5 and 1.5 K below and above 20 K, respectively. Thermopower (S) of the sample was determined by subtracting that of Cu from the slope of ΔE to ΔT. The sample holder used in this study is an improved one[18,37] from that reported previously.[38] Au-Fe(0.07 atom%) chromel thermocouple is used in the present holder instead of Cu-constantan to achieve higher sensitivity below 80 K.

The TAE was measured for $(DMET)_2AuCl_2$ at ambient pressure. To measure the $\mathbf{z}^*$-axis magnetoresistance by the four-probe method, two pairs of annealed gold wires of 10 μm in diameter were attached with gold paste on each crystal surface that is parallel to the most conducting $\mathbf{xy}$ plane, on which gold pads were previously evaporated. The magnetoresistance was measured by applying the magnetic field up to 7 T rotated within the $\mathbf{xy}$ plane at 4.2 and 1.5 K, respectively.

III. RESULTS AND DISCUSSION

A. Thermopower of $(DMET)_2X$

The thermopower of $(DMET)_2X$ is shown in Fig. 1. Among them $(DMET)_2Au(CN)_2$ and $(DMET)_2AuI_2$ undergo the SDW transition at low temperature. Gradual increase in the thermopower toward the $T_{SDW}=24$ and 16 K from higher temperature is followed by its sharp decrease and sign reversal below T_{SDW}. The increase in the thermopower is probably due to the fluctuation of the SDW transition as noted above. The thermopower and the SDW transition of the $(DMET)_2Au(CN)_2$ and $(DMET)_2AuI_2$ are discussed in detail in the literature.[18] The thermopower of $(DMET)_2Au(CN)_2$ shows another anomaly concerning a structural phase transition of higher order at 180 K.[38,39]

$(DMET)_2AuCl_2$, $(DMET)_2IBr_2$, and $(DMET)_2I_3$ are superconducting below $T_c=0.83$, 0.53, and 0.47 K, respectively. No phase transition has been reported for $(DMET)_2AuBr_2$ ($Z=1$) and $(DMET)_2SCN$. Although all the salts show good linear temperature dependence of thermopower in the metallic region as expected for normal metals, each own character is revealed by subtracting linear part of S. Figure 2 shows $\Delta S=S(T)-(S_{300\,K}/300\ K)T$. The thermopower at 300 K, $S_{300\,K}$ is tabulated in Table I. It was

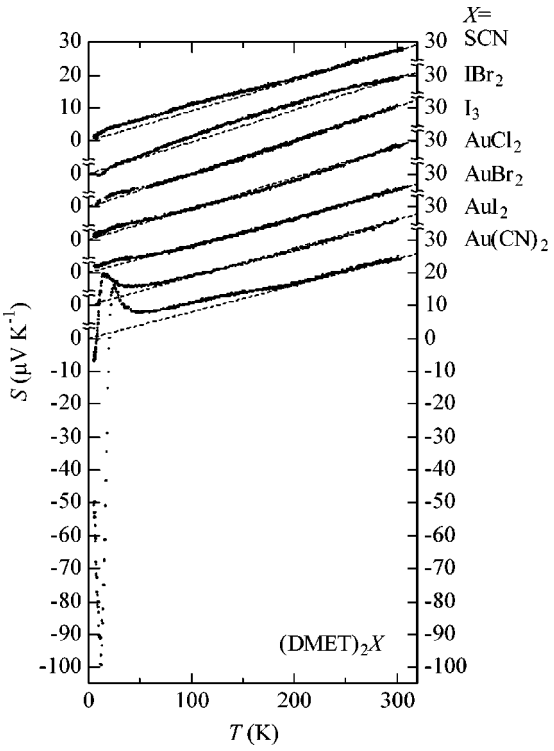

FIG. 1. Thermopower of $(DMET)_2X$, [$X=Au(CN)_2$ (Ref. 18), AuI_2 (Ref. 18), $AuCl_2$, IBr_2, I_3, SCN, and $AuBr_2$ ($Z=1$)]. Each data curve is shifted by a step of 10 μV K^{-1}. Each broken line is drawn to fit itself to the experimental result at 300 K.

found that the present DMET salts are classified into three types based on the similarity of ΔS in the metallic state. The first type of salts are $(DMET)_2AuI_2$, $(DMET)_2AuBr_2$, $(DMET)_2AuCl_2$, and $(DMET)_2I_3$. Their thermopower has quite linear temperature dependence as represented by almost zero ΔS (<1 μ V K^{-1}) above 100 K as in Fig. 2(a). ΔS is almost identical except for $(DMET)_2AuI_2$. Below 100 K, ΔS of these salts gradually increases with decreasing temperature. Although the anomalous enhancement of S (or ΔS) of $(DMET)_2AuI_2$ toward the $T_{SDW}=16$ K is considered to

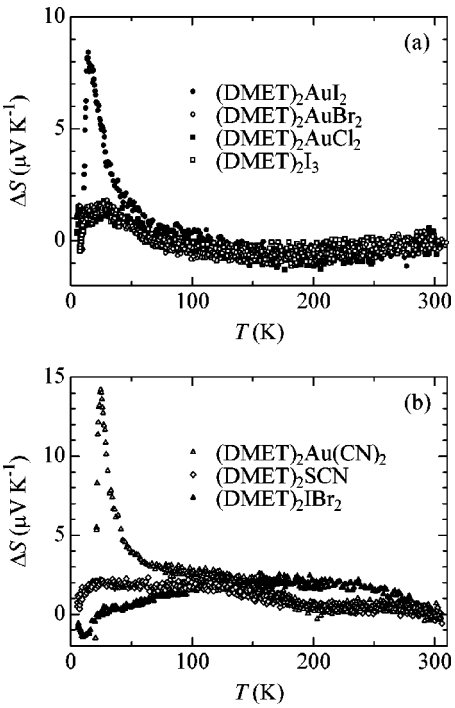

FIG. 2. Deviation of thermopower from the behavior proportional to temperature as represented by the broken lines in Fig. 1.

be critical anomaly of the SDW transition,[18] similar upturn is also seen for $(DMET)_2AuBr_2$, $(DMET)_2AuCl_2$, and $(DMET)_2I_3$ above 25 K. Since $(DMET)_2AuCl_2$ has shallow minimum of the electric resistivity at 3 K, the similarity between the ΔS of $(DMET)_2AuI_2$ and $(DMET)_2AuCl_2$ is not surprising. Indistinguishable ΔS of $(DMET)_2AuBr_2$, $(DMET)_2AuCl_2$, and $(DMET)_2I_3$ as in Fig. 2(a), however, suggests that (i) the fluctuation of the SDW transition also affects the thermopower of $(DMET)_2AuBr_2$ and $(DMET)_2I_3$ which are metallic down to low temperature or (ii) the anomalous enhancement of the thermopower observed for $(DMET)_2AuI_2$ below 100 K ($>5T_{SDW}$) has another mechanism in addition to the critical anomaly that is probably important at temperature close to T_{SDW}.

TABLE I. Thermopower at 300 K ($S_{x,300\,K}$), **x**-axis transfer integral ($|t_x|$) and a lattice constant (x or b) of $(DMET)_2X$.

Group based on $\Delta S_x(T)$	X	$S_{x,300\,K}$ (μ V K^{-1})	$\lvert t_x\rvert$ (eV)	x (or b) (Å)	Note
1	$AuBr_2$	25.2	0.206	7.687[a,b]	Metal
	AuI_2	25.8	0.201	7.724[b,c]	$T_{SDW}=16$ K, $p_c=5$ kbar
	$AuCl_2$	28.4	0.182	7.742[b,d]	$T_{min}=3$ K, $T_c=0.83$ K
	I_3	30.5	0.170	7.769[b,e]	$T_c=0.47$ K
2	$Au(CN)_2$	24.2	0.214	7.710[b,f]	$T_{SDW}=24$ K, $p_c=2.5$ kbar
	SCN	27.5	0.188	7.654[g]	Metal
3	IBr_2	29.1	0.178	7.748[b,h]	$T_c=0.58$ K

[a]Ref. 7.
[b]Ref. 40.
[c]Ref. 41.
[d]Ref. 20.
[e]Ref. 42.
[f]Ref. 43.
[g]Ref. 44.
[h]Ref. 45.

$(DMET)_2Au(CN)_2$ and $(DMET)_2SCN$ are the second type of salts whose ΔS shows stepwise increase at about 180 K in the metallic state by lowering temperature. The anomaly observed for $(DMET)_2Au(CN)_2$ is due to a kind of phase transition of higher order, which also associates the anomalies of electric resistivity[46] and heat capacity[38,39] at about 180 K. A similar anomaly of the electric resistivity was reported for $(DMET\text{-}TSeF)_2Au(CN)_2$,[47] where DMET-TSeF is dimethyl(ethylenedithio)tetraselenafulvalene, an analog of DMET. Thus some kinds of molecular motion of the anion $Au(CN)_2^-$ must play a role in the phase transition, though its detailed mechanism is unclear up to now. Very similar temperature dependence of ΔS of $(DMET)_2Au(CN)_2$ and $(DMET)_2SCN$ with each other above 150 K in Fig. 2(b) implies that such anion-associated phase transition also occurs in $(DMET)_2SCN$.

The estimation of the bandwidth from the thermopower is carried out for the salts of the first and second types with little uncertainty of determining slope of the thermopower. By using Eq. (1),[48] which is based on the tight-binding approximation for one-dimensional (1D) metals, the absolute value of the transfer integral, $|t_x|$ is estimated from S/T or $\partial S/\partial T$.

$$S=\frac{-\pi^2 k_B^2 T}{6|e||t_x|}\frac{\cos\frac{1}{2}\pi\rho}{1-\cos^2\frac{1}{2}\pi\rho}, \tag{1}$$

where k_B is the Boltzmann constant, T the absolute temperature, e the electron charge, $\rho=1.5$ the number of free electrons per donor for the 2:1 salt, respectively.

The third type of $(DMET)_2IBr_2$ shows rather strong change in $\partial S/\partial T$ above 200 K as compared with that of the other DMET salts. Thus the estimated value of $|t_x|$ changes from 0.17 to 0.34 eV from 200 to 300 K for $(DMET)_2IBr_2$ when the numerical derivative of S is used. Here we attempt to estimate $|t_x|$ from S/T at 300 K for comparison of the bandwidth ($\sim 4|t_x|$), where S at 300 K is determined from the least-squares fit to the data above 200 K. These values are listed in Table I with the lattice constant, x (or b) at room temperature for comparison as is discussed in the Sec. III D.

B. Effect of dimerization of donors on thermopower

In the real Q1D metals such as $(DMET)_2X$, donor molecules often dimerizes along its stacking **x** direction. Since the thermopower is closely related to the first and second derivatives of the dispersion relation at Fermi energy, at least, within the relaxation time approximation,[48] the dimerization resulting in the band splitting may affect sign and magnitude of thermopower significantly. It is, however, shown that the deviation of the thermopower of the dimerized system from that of the uniform one is not so large for the 2:1 salts.

The dispersion relations are written for such a system

$$E_k=\pm\sqrt{t_{x1}^2+t_{x2}^2+2|t_{x1}||t_{x2}|\cos kx}, \tag{2}$$

where t_{x1} and t_{x2} are alternating transfer integrals. Then the temperature dependence of the thermopower is expressed as

$$S=\frac{k_B^2\pi^2 T[2(t_{x1}^2+t_{x2}^2)\cos\pi\rho+|t_{x1}||t_{x2}|(3+\cos 2\pi\rho)]\csc^2\pi\rho}{6|e||t_{x1}||t_{x2}|\sqrt{t_{x1}^2t_{x2}^2+2|t_{x1}||t_{x2}|\cos\pi\rho}}, \tag{3}$$

based on the tight-binding approximation as is derived in Appendix A when the upper band is the conduction one ($1<\rho<2$). Figure 3 shows the ratio of Eq. (3) (S_{dimer}) to Eq. (1) ($S_{uniform}$) for $\rho=1.4$, 1.5 (2:1 salts), and 1.6 as a function of Δt under the condition that

$$|t_x|=\bar{t}=(|t_{x1}|+|t_{x2}|)/2, \tag{4}$$

$$|t_{x1}|=\bar{t}+\Delta t, \tag{5}$$

$$|t_{x2}|=\bar{t}-\Delta t. \tag{6}$$

The ratio is simplified as

$$\frac{S_{dimer}}{S_{uniform}}=\frac{1}{\sqrt{1+(\Delta t/\bar{t})^2}}, \tag{7}$$

for $\rho=1.5$. Then the deviation is small (~ 0.1) even in case of strong dimerization ($\Delta t/\bar{t}=0.5$). This is because the Fermi level is in the middle of the upper band and the effect of the band splitting is small. Since the extended Hückel molecular orbital calculation suggests that $\Delta t/\bar{t}$ is between 0.01 and 0.08 for the present $(DMET)_2X$,[49] the deviation is expected to be about 0.3 % at most, though this is not the case if band filling is varied from $\rho=1.5$.

C. Third angular effect of $(DMET)_2AuCl_2$

Figure 4 shows the angular dependence of the magnetoresistance, $\rho_{z*}(\phi)$ of $(DMET)_2AuCl_2$, where ϕ is the angle

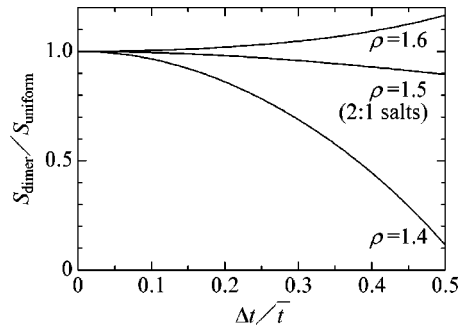

FIG. 3. Ratio of the thermopower of dimerized 1D metal [Eq. (3)] to that of uniform one [Eq. (1)] when degree of the dimerization $(\Delta t/\bar{t})$ is varied under the condition that $|t_x|=\bar{t}=(|t_{x1}|+|t_{x2}|)/2$, $|t_{x1}|=\bar{t}+\Delta t$, and $|t_{x2}|=\bar{t}-\Delta t$.

between the magnetic field and the **x** axis within the **xy** plane. The overall angular dependence of the magnetoresistance is very similar to that of $(DMET)_2I_3$ and $(DMET)_2AuBr_2$. The TAE anomaly is clearly observed between $\phi=\pm 15°$ at 1.5 K and 7.0 T, while its magnitude is rather small at 4.2 K as compared with $(DMET)_2I_3$ (Ref. 21) and $(DMET)_2AuBr_2$.[22] Since $(DMET)_2AuCl_2$ has the shallow resistivity minimum around 3 K, it is considered that the weak TAE anomaly reflects the trace of charge localization at low temperature. The width of the TAE anomaly, $\Delta\phi$ is about 28° and almost the same as that of $(DMET)_2I_3$ (28°) (Ref. 21) and $(DMET)_2AuBr_2$ (27°).[22]

The ratio $|t_x/t_y|$ is estimated as 9.8 from $\Delta\phi=28°$ for $(DMET)_2AuCl_2$ following the procedure reported previously.[22] Since the TAE is closely related to the warping of Q1D Fermi surface, we assume the following anisotropic dispersion relation for the present Q1D metals:

$$E_k=-2|t_x|\cos k_x x-2|t_y|\cos k_y y, \tag{8}$$

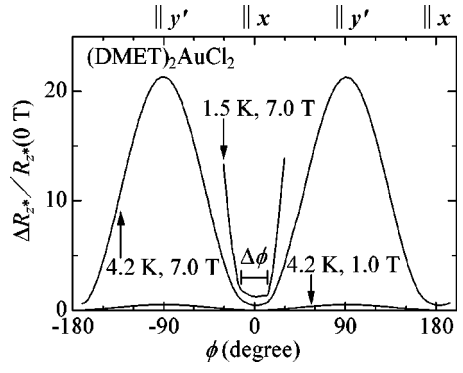

FIG. 4. Angular dependence of the magnetoresistance R_{z*} of $(DMET)_2AuCl_2$ for the electric current along the **z*** axis and the magnetic field rotated within the conducting **xy** plane. The magnetoresistance is normalized by the zero-field value of $R_{z*}=0.275$ and 0.142 Ω at 4.2 and 1.5 K, respectively. The angle, ϕ is zero when the magnetic field is parallel to the most conducting **x** axis. The TAE anomaly is observed between $\pm 15°$ as bends of the magnetoresistance. The definition of the width of the TAE anomaly is illustrated by the bar in the figure.

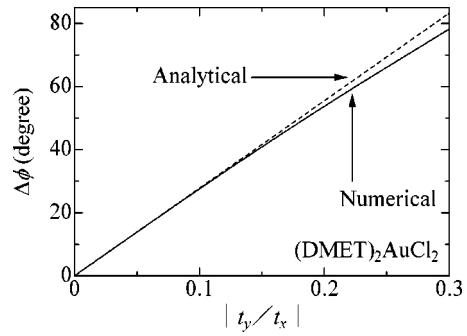

FIG. 5. The width of the TAE anomaly $\Delta\phi$ for $(DMET)_2AuCl_2$ calculated as the sum of the inflection angles of Q1D Fermi surface using the lattice constants at room temperature by varying $|t_y/t_x|$ based on Eq. (8) numerically (solid curve) and from the analytical formula (9) (broken line), respectively.

where t_x and t_y are transfer integrals along the **x** and **y** axes. The slight dimerization of donor molecules along the **x** axis is ignored in addition to the small **z**-axis dispersion. Since $\Delta\phi$ is close to the angle between two normals to the Q1D Fermi surface at two inflection points,[31–33] the dependence of $\Delta\phi$ on $|t_y/t_x|$ is numerically calculated using the lattice constants determined experimentally and the band filling of 3/4 from the 2:1 stoichiometry of the donor and the monovalent anion as shown in Fig. 5 (solid curve). It is noted that the function $\Delta\phi(|t_y/t_x|)$ is independent of how to take the primitive lattice vectors in a Q1D organic metal, because the shape of the Q1D Fermi surface is always identical as far as one neglects the small dimerization along the **x** axis. Now one can determine $|t_y/t_x|$ inversely from the experimental value of $\Delta\phi$. On the other hand, it may be convenient to use an approximated analytical expression of $\Delta\phi$ as derived in Appendix B.

$$\Delta\phi\ \ [\mathrm{rad}]=2\sqrt{2}\,\frac{y}{x}\,\frac{|t_y|}{|t_x|}\sin\gamma. \tag{9}$$

This function is illustrated for $(DMET)_2AuCl_2$ by the broken line in Fig. 5. The ratio $|t_x/t_y|$ is estimated as 9.9 from the lattice constants [$x=b/2=3.871$ Å, $y=a=7.021$ Å, and $\gamma=70.82°$ (Refs. 20,40)] and the experimental value, $\Delta\phi=28°$. The correspondence is fairly good between the values of $\Delta\phi$ estimated by the numerical calculation and the analytical formula by the lowest order of approximation at $|t_x/t_y|\sim 10$.

The solid curve in Fig. 5 is almost the same among the present $(DMET)_2X$. This is because $\Delta\phi$ is related not to the absolute value of the lattice constants but to their ratio y/x which varies $\Delta\phi$ little as compared with $|t_y/t_x|$. This allows us to combine the lattice constants at room temperature and $\Delta\phi$ at low temperature to estimate $|t_y/t_x|$ and, furthermore, to utilize the present method under hydrostatic pressure.[50]

D. Chemical pressure effect on the band parameters

The values listed in Table I are plotted in Fig. 6. It seems that $|t_x|$ (or $S_{x,300\,K}$) and the lattice constant, x have fairly good and reasonable linear relation, namely the smaller x

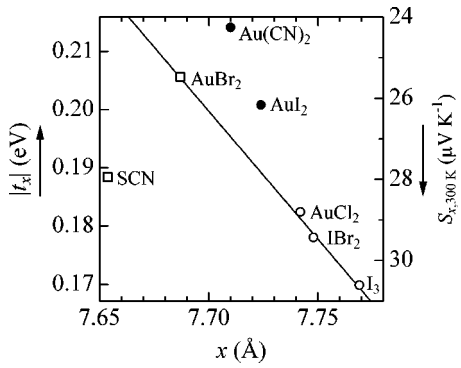

FIG. 6. Thermopower of $(DMET)_2X$ at 300 K, $S_{x,300\ K}$ measured along the **x** axis and transfer integral $|t_x|$ from $S_{x,300\ K}/300$ K using Eq. (1) plotted versus the lattice constant, x $(=b)$ at room temperature. The symbols represent the ground state of $(DMET)_2X$ at low temperature, namely, closed circles, open circles, and squares are for SDW, superconducting, and metallic states, respectively. The solid line is fitted to the points of $(DMET)_2I_3$, $(DMET)_2IBr_2$, and $(DMET)_2AuBr_2$, all of which do not show any sign of the SDW transition.

results in the larger $|t_x|$. The larger $|t_x|$ of $(DMET)_2Au(CN)_2$ (0.23 eV) and $(DMET)_2AuI_2$ (0.24 eV) than that of $(DMET)_2I_3$ (0.21 eV) was previously reported by measuring the polarized reflectance spectra.[51] The change in $|t_x|$ amounts to $\sim$20% at most by the substitution of anions. The solid line in Fig. 6 is fitted to the data points of $(DMET)_2I_3$, $(DMET)_2IBr_2$, and $(DMET)_2AuBr_2$ which do not show any sign of the SDW transition. The donor packing of $(DMET)_2SCN$ is rather dense along the intercolumnar direction reflecting the small size of SCN^- as compared with the other isostructural DMET salts.[44] This probably explains the large deviation of the data point of $(DMET)_2SCN$ from the solid line in Fig. 6. It seems that $(DMET)_2Au(CN)_2$ ($T_{SDW}=24$ K) and $(DMET)_2AuI_2$ ($T_{SDW}=16$ K) also deviates from the solid line and the distance from the solid line depends on T_{SDW}. $(DMET)_2AuCl_2$ has a marginal character between the SDW and superconducting natures with metallic resistivity down to 3 K. It is, therefore, reasonable that $(DMET)_2AuCl_2$ is close to the solid line in Fig. 6.

It is also interesting that $(DMET)_2I_3$, $(DMET)_2IBr_2$, and $(DMET)_2AuCl_2$, which are superconducting at ambient pressure, have large x and small $|t_x|$ because this implies the small density of states at Fermi energy. There is, however, unusual relation between T_c and $|t_x|$ among these salts, namely, higher T_c for the salt with wider bandwidth. This implies that T_c is not determined only by the density of states that is simply deduced from $|t_x|$.

As for the dimensionality, it has been revealed that $|t_x/t_y|=$ 9.8, 9.7 and 10 for $(DMET)_2AuCl_2$ (present study), $(DMET)_2I_3$, and $(DMET)_2AuBr_2$, respectively. This means that the dimensionality is almost the same or very slightly lower (more 1D) for smaller lattice constant x for these three salts, whose electric resistivity shows different temperature dependence at low temperature from one another. It is, however, difficult to find simple chemical pressure effect on the ground state of these DMET salts through the bandwidth and/or the dimensionality. Namely, $(DMET)_2AuCl_2$, which shows the resistivity minimum, has the magnitude of the bandwidth between that of $(DMET)_2I_3$ and $(DMET)_2AuBr_2$ both of which show no sign of SDW, while no significant difference is found for their dimensionality.

Recent development of the theory on the SDW transition[15] predicts that the SDW becomes unstable by the increase in magnitude of the bandwidth as well as in dimensionality. Thus the largest $|t_x|$ for $(DMET)_2AuBr_2$ and the largest $|t_y/t_x|$ for $(DMET)_2I_3$ among these salts may explain that $(DMET)_2AuBr_2$ and $(DMET)_2I_3$ do not undergo the SDW transition. The following inequality, however, excludes this simple picture. The standard theory[12,13] predicts the relation between the amplitude of the band along the k_y axis $(2\varepsilon_0)$ and the SDW gap $(2M_0)$ at 0 K that

$$\varepsilon_0 < M_0 \tag{10}$$

as the stability condition of the SDW. Here ε_0 and M_0 are expressed as

$$\varepsilon_0 = \frac{t_y^2 \cos X_F}{2|t_x| \sin^2 X_F}, \tag{11}$$

$$M_0 = 2D \exp\left(-\frac{1}{N(0)I}\right), \tag{12}$$

$$D = \frac{4|t_x| \sin^2 X_F}{\cos X_F}, \tag{13}$$

$$N(0) = \frac{N}{4\pi |t_x| \sin X_F}, \tag{14}$$

$$I = U/N, \tag{15}$$

$$X_F = x k_{x,F}, \tag{16a}$$

$$= \pi/4 \quad (1/4\text{-filled case}) \tag{16b}$$

and N is the number of sites and U the electron correlation energy, respectively. Then Eq. (10) is reduced to

$$8\left(\frac{t_x}{t_y}\right)^2 \exp\left(-\frac{2\sqrt{2}\pi |t_x|}{U}\right) > 1. \tag{17}$$

This condition is fulfilled in the area between the solid curves and $|t_x|$ axis as shown in Fig. 7 for several values of U. The band parameters of $(DMET)_2I_3$, $(DMET)_2AuCl_2$, and $(DMET)_2AuBr_2$ are also plotted and almost on the broken line of $|t_y|=|t_x|/10$. It is clear that there is no combination of the values of $|t_x|$, $|t_y|$ and U for that only $(DMET)_2AuCl_2$ is expected to undergo the SDW transition. It is probably one aspect of the reality that the largest bandwidth for $(DMET)_2AuBr_2$ and the largest dimensionality for $(DMET)_2I_3$ among the three salts are the reason why each of $(DMET)_2AuBr_2$ and $(DMET)_2I_3$ does not undergo the SDW transition. Another important band parameter is probably t_z

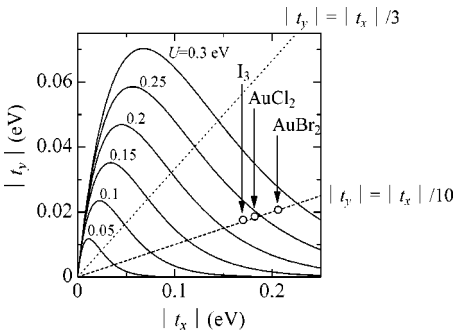

FIG. 7. The condition where the SDW state is stable at 0 K based on the mean-field theory (Refs. 12,13). Equation (17) is fulfilled within the area between each curves and t_x-axis for several values of on-site Coulomb energy U. The broken line is $|t_y| = |t_x|/10$ and the solid circles show the experimental values of $(|t_x|,|t_y|)$ for $(DMET)_2I_3$, $(DMET)_2AuCl_2$, and $(DMET)_2AuBr_2$ $(Z=1)$. The dotted line is $|t_y|=|t_x|/3$ below which the open Fermi surface is expected when Eq. (8) is assumed.

as suggested by the suppression of the SDW transition of $(TMTSF)_2PF_6$ by the uniaxial strain along the **z***- (or **c***-) axis.[14]

It is important to note again that $(DMET)_2AuCl_2$ is not isostructural to the other $(DMET)_2X$ studied. The DMET molecules in the neighboring columns interact with each other in the different manner in $(DMET)_2AuCl_2$ from that in the others. Thus one may consider that using only $|t_y/t_x|$ as an adjustable parameter is too simple to describe the denesting feature of $(DMET)_2X$ and its analogs as has been pointed out in the standard theory in case of multiple-transverse interactions.[13,52,53] The temperature dependence of S in Fig. 1 and ΔS in Fig. 2(a), however, strongly suggests that the electronic system of $(DMET)_2AuCl_2$, $(DMET)_2I_3$, and $(DMET)_2AuBr_2$ is very similar to one another. Furthermore, since the TAE directly observes the degree of Fermi surface warping and it is almost the same for the three salts, the estimated dimensionality probably reflects one aspect of the denesting feature of their electronic system.

IV. CONCLUSION

We applied a new method to evaluate both $|t_x|$ and $|t_y|$ of Q1D $(DMET)_2X$ by combining the thermopower and magnetoresistance measurements. Fairly good linearity between $|t_x|$ and the lattice constant (x) was found for the salts that is metallic at low temperature. The magnitude of $|t_x|$ changes by 25% at most by the anion substitution, while $|t_y/t_x|$ is almost the same among the DMET salts that show different temperature dependence of the electric resistivity at low temperature. This suggests the chemical pressure effect on the ground state of the Q1D organic conductors works as the change in the bandwidth rather than that in the dimensionality at least in a family of materials. It was found that the standard theory of the SDW transition does not explain the different ground states of $(DMET)_2I_3$, $(DMET)_2AuBr_2$, and $(DMET)_2AuCl_2$ from one another when their $|t_x|$ and $|t_y/t_x|$ are compared. The estimation of $|t_z|$ is probably needed to understand the stability of the SDW from the view point of the denesting of the Q1D Fermi surface.

ACKNOWLEDGMENTS

This work was partially supported by Fund for Special Project at Tokyo Metropolitan University, and Grant-in-Aid for Specially Promoted Research (Grant No. 63060004) from the Ministry of Education, Science and Culture and also carried out as a part of ''Research for the Future'' project, Grant No. JSPS-RFTF97P00105, supported by the Japan Society for the Promotion of Science.

APPENDIX A: THERMOPOWER OF DIMERIZED 1D METALS BASED ON THE TIGHT-BINDING APPROXIMATION

By solving the Boltzmann equation under the relaxation time approximation for the 1D system, one obtains the following expression for the temperature dependence of thermopower:[48]

$$S=-\frac{\pi^2 k_B^2 T}{3|e|}\left[\frac{E_k''}{(E_k')^2}+\frac{\tau'(E)}{\tau(E)}\right]_{\varepsilon=\mu}. \tag{A1}$$

Since the dispersion relation for the dimerized 1D system is given as

$$E_k=\pm\sqrt{q}, \tag{A2}$$

$$q=t_{x1}^2+t_{x2}^2+2|t_{x1}||t_{x2}|\cos k_x x, \tag{A3}$$

by the tight-binding approximation, where t_{x1} and t_{x2} are transfer integrals and x is the lattice constant, the first and second derivatives of E_k are calculated as

$$E_k'=-\frac{x|t_{x1}||t_{x2}|\sin k_x x}{\sqrt{q}}, \tag{A4}$$

$$E_k''=-\frac{x^2|t_{x1}||t_{x2}|\cos k_x x}{\sqrt{q}}-\frac{x^2|t_{x1}||t_{x2}|\sin^2 k_x x}{q^{3/2}}, \tag{A5}$$

for the upper band and similarly for the lower one. When one neglects the energy dependence of τ around the Fermi level, the thermopower is expressed as follows by using the linear relation between $k_x x$ and the number of carriers per site $(0\leqslant\rho\leqslant 2)$.

$$S=\pm\frac{k_B^2\pi^2 T[2(t_{x1}^2+t_{x2}^2)\cos\pi\rho+|t_{x1}||t_{x2}|(3+\cos 2\pi\rho)]\csc^2\pi\rho}{6|e||t_{x1}||t_{x2}|\sqrt{t_{x1}^2t_{x2}^2+2|t_{x1}||t_{x2}|\cos\pi\rho}}. \tag{A6}$$

The plus and minus signs are taken for $\rho>1$ and <1, respectively. This equation is reduced to Eq. (1) when $t_{x1}=t_{x2}$ and to Eq. (A7) for the 3/4(1/4)-filled case, respectively.

$$S=\pm\frac{k_B^2\pi^2T}{3|e|\sqrt{t_{x1}^2+t_{x2}^2}}. \tag{A7}$$

APPENDIX B: INFLECTION ANGLE OF Q1D FERMI SURFACE IN THE TRICLINIC SYSTEM

Starting with a normalized dispersion relation within a two-dimensional model

$$\varepsilon\equiv E/(2|t_x|)=-\cos k_x-d\cos k_y r, \tag{B1}$$

$$d=|t_y/t_x|, \tag{B2}$$

$$r=y/x, \tag{B3}$$

one can obtain an analytical expression of the two inflection angles ϕ_i of the Q1D Fermi surface of a material with lattice constants x, y, and γ, and transfer integrals t_x and t_y between the nearest neighbor sites along the **x** and **y** axes, respectively. Trace of the Q1D Fermi surface is drawn by solving Eq. (B1) when $\varepsilon=\varepsilon_F$. The solutions are

$$k_{x,F}=\pm\cos^{-1}(-\varepsilon_F-d\cos k_y r). \tag{B4}$$

The inflection angle ϕ_i is one between the normal to the Fermi surface at the inflection point and the most conducting **x** axis within the **xy** plane. The slope of the Fermi surface $\partial k_{X,F}/\partial k_Y$ is calculated as

$$\frac{\partial k_{X,F}}{\partial k_Y}=\frac{\partial k_{X,F}}{\partial k_{x,F}}\frac{\partial k_{x,F}}{\partial k_y}\frac{\partial k_y}{\partial k_Y} \tag{B5a}$$

$$=\sin\gamma_k\frac{\partial k_{x,F}}{\partial k_y}\left(\frac{\partial k_{x,F}}{\partial k_y}\cos\gamma_k+1\right)^{-1}, \tag{B5b}$$

$$\frac{\partial k_{x,F}}{\partial k_y}=\frac{rd\sin k_y r}{\sqrt{1-(-\varepsilon_F-d\cos k_y r)^2}}, \tag{B6}$$

$$k_{X,F}=k_{x,F}\sin\gamma_k, \tag{B7}$$

$$k_Y=k_{x,F}\cos\gamma_k+k_y, \tag{B8}$$

$$\gamma_k=\pi-\gamma, \tag{B9}$$

where the **X** and **Y** axes refer the Cartesian coordinate and the latter is taken to be parallel to the **y** axis. The maximum and the minimum of $\partial k_{X,F}/\partial k_Y$ are calculated based on the condition $\partial^2 k_{X,F}/\partial k_Y^2=0$. Then ϕ_i is calculated as follows:

$$\phi_i=\tan^{-1}\left(\left.\frac{\partial k_{X,F}}{\partial k_Y}\right|_{\max,\min}\right)=\tan^{-1}\left(\frac{s\sin\gamma_k}{\pm2+s\cos\gamma_k}\right), \tag{B10}$$

$$s=\sqrt{2}r\sqrt{1-\varepsilon_F^2+d^2-\sqrt{-4\varepsilon_F^2d^2+(-1+\varepsilon_F^2+d^2)^2}}. \tag{B11}$$

When ε_F is approximated to be $\varepsilon_{\mathrm{F,1D}}=1/\sqrt{2}$, that is the Fermi energy for the 3/4-filled band in the pure 1D case, Eq. (B11) is simplified as

$$s=r\sqrt{1+2d^2-\sqrt{1-12d^2+4d^4}}. \tag{B12}$$

The second term of Taylor's series of Eq. (B10) with Eq. (B12) gives asymmetrical critical angles and $\Delta\phi$ for the triclinic system

$$\phi_i=\pm\sqrt{2}rd\sin\gamma_k-2r^2d^2\cos\gamma_k\sin\gamma_k, \tag{B13}$$

$$\Delta\phi=2\sqrt{2}rd\sin\gamma_k=2\sqrt{2}rd\sin\gamma. \tag{B14}$$

This result matches with that obtained for the orthorhombic system where $\gamma=\pi/2$ (Ref. 31).

*Electronic address: yoshino@sci.osaka-cu.ac.jp

[1] K. Murata, K. Kikuchi, T. Takahashi, Y. Honda, K. Saito, K. Kanoda, T. Tokiwa, H. Anzai, T. Ishiguro, and I. Ikemoto, J. Mol. Electron. **4**, 173 (1988).

[2] T. Ishiguro, K. Yamaji, and G. Saito, *Organic Superconductors*, 2nd ed. (Springer-Verlag, Berlin, 1998), pp. 221–230.

[3] K. Kikuchi, M. Kikuchi, T. Namiki, H. Saito, I. Ikemoto, K. Murata, T. Ishiguro, and K. Kobayashi, Chem. Lett. **1987**, 931 (1987).

[4] Y. Nogami, M. Tanaka, S. Kagoshima, K. Kikuchi, K. Saito, I. Ikemoto, and K. Kobayashi, J. Phys. Soc. Jpn. **56**, 3783 (1987).

[5] K. Kikuchi, K. Murata, Y. Honda, T. Namiki, K. Saito, H. Anzai, K. Kobayashi, T. Ishiguro, and I. Ikemoto, J. Phys. Soc. Jpn. **56**, 4241 (1987).

[6] K. Kikuchi, K. Murata, Y. Honda, T. Namiki, K. Saito, T. Ishiguro, K. Kobayashi, and I. Ikemoto, J. Phys. Soc. Jpn. **56**, 3436 (1987).

[7] K. Kikuchi, Y. Honda, Y. Ishikawa, K. Saito, I. Ikemoto, and K. Kobayashi, Solid State Commun. **66**, 405 (1988).

[8] T. Ishiguro, K. Yamaji, and G. Saito, *Organic Superconductors* (Ref. 2), pp. 58–64.

[9] T. Takahashi, D. Jérome, and K. Bechgaard, J. Phys. (France) Lett. **43**, 565 (1982).

[10] S. Kagoshima, T. Yasunaga, T. Ishiguro, H. Anzai, and G. Saito, Solid State Commun. **46**, 867 (1983).

[11] H. Schwenk, K. Andres, and F. Wudl, Phys. Rev. B **29**, 500 (1984).

[12] K. Yamaji, J. Phys. Soc. Jpn. **51**, 2787 (1982).

[13] T. Ishiguro, K. Yamaji, and G. Saito, *Organic Superconductors* (Ref. 2) pp. 96–111.

[14] F. Guo, K. Murata, A. Oda, Y. Mizuno, and H. Yoshino, J. Phys. Soc. Jpn. **69**, 2164 (2000).

[15] M. Miyazaki, K. Kishigi, and Y. Hasegawa, J. Phys. Soc. Jpn. **69**, 997 (2000).

[16] K. Saito, H. Yoshino, K. Kikuchi, I. Ikemoto, and K. Kobayashi, Synth. Met. **41-43**, 2395 (1991).

[17] K. Murata, K. Kikuchi, Y. Honda, T. Komazaki, K. Saito, K. Kobayashi, and I. Ikemoto, in *The Physics and Chemistry of Organic Superconductors*, edited by G. Saito and S. Kagoshima (Springer-Verlag, Berlin, 1990), pp. 234–237.
[18] K. Saito, H. Yoshino, K. Kikuchi, K. Kobayashi, and I. Ikemoto, J. Phys. Soc. Jpn. **62**, 1001 (1993).
[19] C. Bourbonnais and D. Jérome, Science **281**, 1155 (1998).
[20] Y. Ishikawa, K. Saito, K. Kikuchi, I. Ikemoto, K. Kobayashi, and H. Anzai, Acta Crystallogr., Sect. C: Cryst. Struct. Commun. **46**, 1652 (1990).
[21] H. Yoshino, K. Saito, K. Kikuchi, H. Nishikawa, K. Kobayashi, and I. Ikemoto, J. Phys. Soc. Jpn. **64**, 2307 (1995).
[22] H. Yoshino, K. Saito, H. Nishikawa, K. Kikuchi, K. Kobayashi, and I. Ikemoto, J. Phys. Soc. Jpn. **66**, 2410 (1997).
[23] A. G. Lebed, Pis'ma Zh. Éksp. Teor. Fiz. **43**, 137 (1986) [JETP Lett. **43**, 174 (1986)].
[24] A. G. Lebed and P. Bak, Phys. Rev. Lett. **63**, 1315 (1989).
[25] M. Naughton, O. Chung, L. Chiang, S. Hannahs, and J. Brooks, in *Electrical, Optical, and Magnetic Properties of Organic Solid-State Materials*, edited by L. Y. Chiang, D. O. Cowan, and P. Chaikin, Mater. Res. Soc. Symp. Proc. No. 173 (Materials Research Society, Pittsburgh, 1990), p. 257.
[26] T. Osada, A. Kawasumi, S. Kagoshima, N. Miura, and G. Saito, Phys. Rev. Lett. **66**, 1525 (1991).
[27] M. Naughton, O. Chung, M. Chaparala, X. Bu, and P. Coppens, Phys. Rev. Lett. **67**, 3712 (1991).
[28] W. Kang, S. T. Haanas, and P. M. Chaikin, Phys. Rev. Lett. **69**, 2827 (1992).
[29] T. Osada, S. Kagoshima, and N. Miura, Phys. Rev. B **46**, 1812 (1992).
[30] G. M. Danner, W. Kang, and P. M. Chaikin, Phys. Rev. Lett. **72**, 3714 (1994).
[31] T. Osada, S. Kagoshima, and N. Miura, Phys. Rev. Lett. **77**, 5361 (1996).
[32] A. G. Lebed and N. N. Bagmet, Synth. Met. **85**, 1493 (1997).
[33] A. G. Lebed and N. N. Bagmet, Phys. Rev. B **55**, R8654 (1997).
[34] I. J. Lee and M. J. Naughton, Phys. Rev. B **57**, 7423 (1998).
[35] H. Yoshino and K. Murata, J. Phys. Soc. Jpn. **68**, 3027 (1999).
[36] T. Osada, N. Kami, R. Kondo, and S. Kagoshima, Synth. Met. **103**, 2024 (1999).
[37] H. Yoshino, K. Saito, K. Murata, and I. Ikemoto, Netsu Sokutei **27**, 77 (2000).
[38] K. Saito, H. Kamio, Y. Honda, K. Kikuchi, K. Kobayashi, and I. Ikemoto, J. Phys. Soc. Jpn. **58**, 4093 (1989).
[39] K. Saito, H. Kamio, K. Kikuchi, K. Kobayashi, and I. Ikemoto, J. Phys.: Condens. Matter **1**, 8823 (1989).
[40] J. M. Williams, J. R. Ferraro, R. J. Thorn, K. D. Carlson, U. Geiser, H. H. Wang, A. M. Kini, and M.-H. Wahangbo, *Organic Superconductors (Including Fullerenes)* (Prentice Hall, New Jersey, 1992), p. 83.
[41] Y. Ishikawa, K. Kikuchi, K. Saito, I. Ikemoto, and K. Kobayashi, Acta Crystallogr., Sect. C: Cryst. Struct. Commun. **45**, 572 (1989).
[42] M. Z. Aldoshina, L. O. Atovmyan, L. M. Gol'denberg, O. N. Krasochka, R. N. Lyubovskaya, R. B. Lyubovskii, and M. L. Khidekel', Dokl. Akad. Nauk SSSR **289**, 1140 (1986) [Phys. Chem. **289**, 689 (1986).
[43] K. Kikuchi, Y. Ishikawa, K. Saito, I. Ikemoto, and K. Kobayashi, Acta Crystallogr., Sect. C: Cryst. Struct. Commun. **44**, 466 (1988).
[44] The crystal structure of $(DMET)_2SCN$ has not been fully solved due to orientational disorder of SCN^-. The crystal data for the DMET lattice of $(DMET)_2SCN$ are triclinic, space group $P\bar{1}$, $Z=1$, $a=6.7259$ Å, $b=7.6537$ Å, $c=14.7002$ Å, $\alpha=79.02°$, $\beta=83.75°$, $\gamma=76.60°$, $V=721.0$ Å^3. The final R values, $R;R_w=0.0737;0.1945$ were obtained for 2594 unique diffractions ($|F_o|>4\sigma(F_o)$). Packing pattern of the DMET molecules is similar to that of $(DMET)_2AuI_2$ and $(DMET)_2I_3$. There are four intercolumnar short contacts between calcogen atoms (S-S or Se-S), while the other isostructural DMET salts have three.
[45] K. Kikuchi, Y. Ishikawa, K. Saito, I. Ikemoto, and K. Kobayashi, Synth. Met. **27**, B391 (1988).
[46] K. Kikuchi, K. Murata, M. Kikuchi, Y. Honda, T. Takahashi, T. Oyama, I. Ikemoto, T. Ishiguro, and K. Kobayashi, Jpn. J. Appl. Phys. Suppl. **26**, 1369 (1987).
[47] R. Kato, S. Aonuma, Y. Okano, H. Sawa, M. Tamura, and M. Kinoshita, Synth. Met. **61**, 199 (1993).
[48] P. M. Chaikin, R. L. Greene, S. Etemad, and E. Engler, Phys. Rev. B **13**, 1627 (1976).
[49] Y. Ishikawa, M.Sc. thesis, Tokyo Metropolitan University, 1989.
[50] H. Yoshino, A. Oda, K. Murata, H. Nishikawa, K. Kikuchi, and I. Ikemoto, Synth. Met. **120**, 885 (2001).
[51] K. Kikuchi, K. Neriishi, K. Miyazaki, K. Saito, I. Ikemoto, and K. Kobayashi, Synth. Met. **41-43**, 2275 (1991).
[52] K. Yamaji, J. Phys. Soc. Jpn. **53**, 2189 (1984).
[53] K. Yamaji, J. Phys. Soc. Jpn. **55**, 860 (1986).